Room-Temperature Quantum Coherence and Rabi Oscillations in Vanadyl Phthalocyanine: Toward Multifunctional Molecular Spin

Room Temperature Quantum Coherence and Rabi Oscillations in Vanadyl Phthalocyanine: Toward Multifunctional Molecular Spin Qubits

Matteo Atzori,† Lorenzo Tesi,† Elena Morra,‡ Mario Chiesa,‡ Lorenzo Sorace,† and Roberta Sessoli*,†

† Dipartimento di Chimica "Ugo Schiff" & INSTM RU, Università degli Studi di Firenze, Via della Lastruccia 3, I50019 Sesto Fiorentino (Firenze), Italy.

‡ Dipartimento di Chimica & NIS Centre, Università di Torino, Via P. Giuria 7, I10125 Torino, Italy.

Supporting Information Placeholder

ABSTRACT: Here we report the investigation of the magnetic relaxation and the quantum coherence of vanadyl phthalocyanine, VOPc, a multifunctional and easy-processable potential molecular spin qubit. VOPc in its pure form (**1**) and its crystalline dispersions in the isostructural diamagnetic host TiOPc in different stoichiometric ratios, namely VOPc:TiOPc 1:10 (**2**) and 1:1000 (**3**), were investigated via a multitechnique approach based on the combination of alternate current (AC) susceptometry, continuous wave (CW) and pulsed electron paramagnetic resonance (EPR) spectroscopy. AC susceptibility measurements revealed a linear increase of the relaxation rate with temperature up to 20 K, as expected for a direct mechanism, but τ remains slow over a very wide range of applied static field values (up to ca. 5 T). Pulsed EPR spectroscopy experiments on **3** revealed quantum coherence up to room temperature with T_m ca. 1 μs at 300 K, representing the highest value obtained to date for molecular electronic spin qubits. Rabi oscillations are observed in this nuclear spin-active environment (^{1}H and ^{14}N nuclei) at room temperature also for **2**, indicating an outstanding robustness of the quantum coherence in this molecular semiconductor exploitable in spintronic devices.

In the development of spin-based information technology magnetic molecules represent particularly versatile building blocks as they can serve for the realization of both "static" and "dynamic" components of a potential quantum computer.[1] While single-molecule magnets (SMMs) show magnetic bistability resulting from magnetic anisotropy and large spin,[2] molecules with lower spin values can be exploited in quantum computation as quantum bits, or qubits.[3] A qubit is a two states quantum-mechanical system able to be placed in a state of coherent superposition of these levels. Physical realizations of qubits can be found in superconductive circuits, trapped ions, photons, *etc.*[1,4] Nuclear and electronic spins are also interesting because their superposition of spin states can be realized by pulsed magnetic resonance techniques. The most investigated electronic spin systems are nitrogen-vacancy pairs in diamonds[5] or defects in silicon[6] or silicon carbide.[7] Polynuclear metal complexes, [3,8] in particular ferrimagnetic rings,[9] have been also investigated for the possibility to use synthetic chemistry to obtain multi-bit systems. Only recently, molecular spin systems have become really competitive. The realization of a qubit requires, in fact, the accomplishment of stringent and antithetic requirements known as Di Vincenzo criteria.[10] If molecules are better suited to satisfy some of them, like addressing and control of qubits entanglement, the short lifetime of the quantum superposition of states, T_m, has up to now posed some limitations in their use as qubits. Recently promising results have been obtained on simple $S = ½$ complexes. [11,12] Remarkably, mononuclear V^{IV} complexes with nuclear spin-free ligands like dithiolenes,[13] when dispersed in nuclear spin-free solvents like CS_2, can attain, at low temperature, T_m of the order of the millisecond,[14] a value comparable to those observed for vacancies in extended lattices. Their use at room temperature is however hampered by the rapid decrease, on increasing the temperature, of the spin-lattice relaxation time, T_1, which acts as a limiting factor for T_m.

In a recent investigation we have shown that AC susceptibility can flank pulsed EPR techniques to identify species that show slow spin-lattice relaxation as potential spin qubits.[15] A vanadyl complex with β-diketonate ligands has revealed remarkable T_m despite the proton rich ligands, and, more interestingly, a long T_1 over a wide range of temperature and applied magnetic fields.

Keeping in mind the growing interest to address single molecules on surfaces exploiting their electric conductance, we focused our attention on vanadyl phthalocyanine, VOPc. This system exhibits the expected electronic and structural features to behave as a molecular spin qubit combined with other technologically relevant physical properties, such as extrinsic and photoinduced semiconductivity[16] and the ability of being deposited on different surfaces in oriented dispositions,[17] fundamental requisites for a suitable processability and incorporation of these materials in real devices. The high stability of the diamagnetic analogue, titanyl phthalocyanine, TiOPc, allows the preparation of crystalline materials with different percentage of paramagnetic component diluted in the diamagnetic host leading to two important advantages: *i)* reduce the interactions between electronic magnetic mo-

ments, that significantly increases the T_2 relaxation time,[18] and *ii)* extend the investigation up to room temperature, avoiding the melting of frozen solutions. We have thus investigated the magnetic relaxation and the quantum coherence of VOPc in its pure form (**1**) and its crystalline dispersions in the isostructural diamagnetic host TiOPc in different molar ratios, 1:10 (**2**) and 1:1000 (**3**), through a multitechnique approach based on the combination of AC susceptometry, and CW and pulsed EPR spectroscopies.

VOPc is a non-planar metal-phthalocyanine in which the vanadyl ion VO^{2+}, coordinated by four nitrogen donor atoms of the dianionic phthalocyaninato ligand, points out of the plane of the ligand. The coordination geometry around the pentacoordinated V^{IV} ion is a distorted square pyramid with the metal slightly above the basal plane (0.575(1) Å).[19] The apical position is occupied by an oxo ligand which forms a double bond with the V^{IV} ion having a V=O distance of 1.580(3) Å, whereas the V–N bond lengths are in the 2.008(7)-2.034(7) Å range (Figure 1).

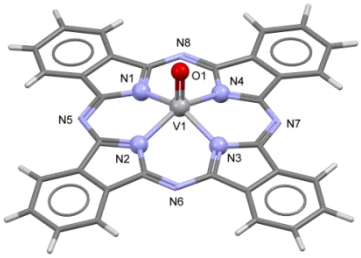

Figure 1. Molecular structure of VOPc with principal atoms labelling scheme and coordination geometry of the V^{IV} ion highlighted.

The presence of such short V=O bond distance is responsible for a *d*-orbitals splitting that leaves the d_{xy} orbital lowest in energy and well separated from the other orbitals, making this molecule a perfect two levels potential molecular qubit. VOPc and its diamagnetic analogue TiOPc exhibit a rich polymorphism and crystallize in more than four different structural phases showing slight different crystal packings (Type I–IV polymorphs).[20] Type II was selected because π–π stacked supramolecular dimers are absent in the crystal structure and is the preferred one for VOPc (Figure S1). Moreover, TiOPc can be conveniently converted in this structural phase by dissolution in a 1:4 mixture of CF_3COOH:CH_2Cl_2 and successive precipitation in *iso*-propanol (see SI).[20] Powder X-ray diffraction analyses performed on polycrystalline samples show structural phase homogeneity for all the investigated samples and a good agreement between experimental and simulated patterns (Figure S2).

Compounds **1** and **2** were investigated by AC susceptometry in order to get deeper insights on their magnetization dynamics. The thermal variation of the magnetic susceptibility in a zero static magnetic field reveals no imaginary component of the susceptibility (χ'') in the whole investigated T range (1.9–40 K). When a small static magnetic field (> 40 mT) is applied, slow magnetic relaxation is observed with appearance of a peak in the imaginary component of the susceptibility and a concomitant decrease of the real part (χ') (Figures S3-S10). Both **1** and **2** under a static magnetic field (B) of 0.2 T show slow relaxation of the entire magnetization, so that this field, and a higher one (1 T), were selected to investigate the T dependence of the relaxation time (τ). The frequency dependence of χ'' are well reproduced with the Debye model (Figures S3-S10) and the extracted values of τ as a function of T for the two selected fields are reported in Figure 2a.

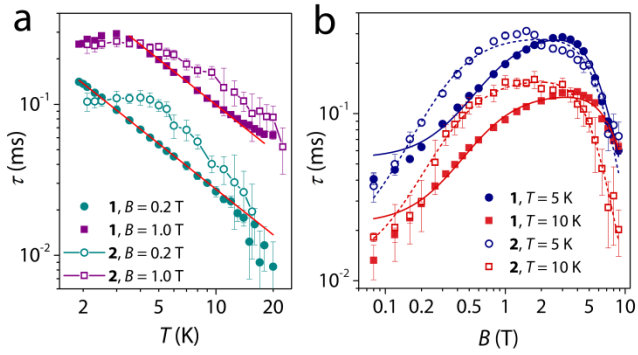

Figure 2. (a) T and (b) B dependence of τ extracted from AC susceptibility measurements on **1** and **2** at different applied static magnetic field values and temperatures (see legends). Solid and dashed lines are the best-fits of the models.

Figure 2a shows that **1** exhibits up to 20 K a τ dependence typical of the direct mechanism of relaxation in absence of phonon-bottleneck effects.[21] The field dependence of τ in this T range (Figure 2b) shows an increase up to ca. 3 T while the rapid decrease expected for the direct mechanism is only visible above 5 T. The non-monotonous behavior is due to two antagonist effects of the magnetic field. An isolated S = ½ spin in zero field should not be able to relax due to time-reversal symmetry, but spin-spin and spin-nuclei interactions promote a rapid relaxation, as recently discussed for a Co^{II} pseudo S = ½ spin system.[22] The latter mechanisms are suppressed when the magnetic field splits the energy of the doublet, similarly to the phenomenon of resonant quantum tunneling in SMMs.[2] On the other hand, the larger is the energy separation of the doublet the more efficient is the spin-phonon direct mechanism providing $\tau^{-1} \propto B^4$. In general, fields weaker than 1 T are sufficient to accelerate the relaxation.[23] The two mechanisms can be taken into account in a phenomenological model described by the following equation:[24]

$$\tau^{-1} = cB^4 + d\frac{e(f+B^2)}{ef+B^2} \qquad (1)$$

The first term considers the typical field dependence of a direct process while in the second term, d represents the zero-field relaxation rate, e is a parameter related to the concentration, and f is a parameter proportional to the square of the internal field generated by neighboring spins. The best-fit parameters are reported in Table S1. It is interesting to notice that f decreases significantly passing from **1** to **2**, in agreement with the reduction upon dilution of the internal field. The increase of the zero field relaxation rate, which is not expected, appears however as an artifact of the poor reproduction of the low field data, as testified by the large errors. As a result, τ increases much faster in moderate field in **2**, indicating that both spin-spin and hyperfine interactions are active in promoting relaxation in weak applied fields. A comparison with a recent report on the compound $VO(dpm)_2$ (dpm^- is the anion of dipivaloylmethane)[15] shows, in both cases, a remarkable wide field range where τ remains

long, suggesting that the double V-O bond increases the energy of vibrational modes relevant for the magnetic relaxation. We can notice that τ is in general shorter for VOPc and the maximum is observed at higher fields, in agreement with the additional contributions to the spin relaxation of the nitrogen nuclear spins directly coordinated to the V^{IV} ion. This could also justify the low temperature saturation of τ, not detected in $VO(dpm)_2$.

The CW-EPR X-band spectra of compounds **1-3** at 300 K and 5 K are reported in Figure S11. **1** shows a broad spectrum very likely due to the presence of an extensive network of intermolecular interactions between paramagnetic molecules.[19] The 1:10 crystalline dispersion of VOPc in TiOPc (**2**) dramatically changes the EPR spectrum, which reveals already at room temperature the expected hyperfine splitting due to the coupling with the nuclear spin of ^{51}V (I = 7/2, natural abundance: 99.75%). By lowering the concentration of the paramagnetic component to 1:1000 (**3**), the superhyperfine spectral features due to the further coupling with the nuclear spins (I = 1) of the chelating ^{14}N nuclei become visible (Figure 3a).[25] As far as the position of the resonance lines are concerned, no significant variations are observed between **2** and **3**, thus confirming that VOPc retains the same molecular geometry and environment (Figure S11).

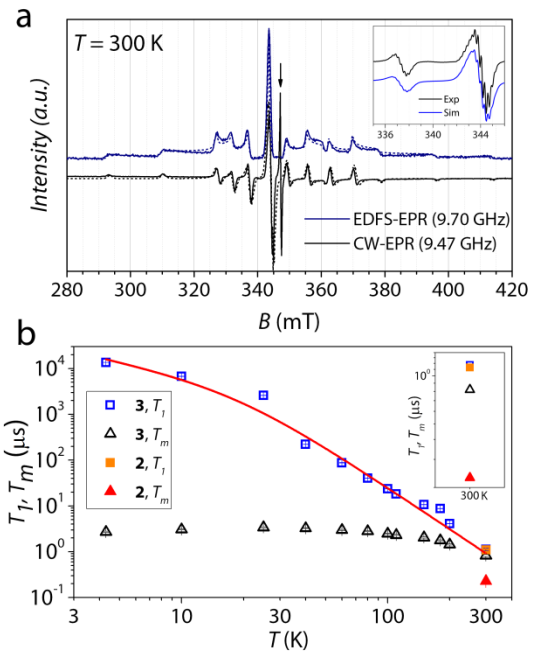

Figure 3. (a) EDFS- and CW-EPR X-band spectra for **3**. CW data were translate for ease of comparison with EDFS data. Short-dashed lines are the best-simulations. Inset shows the CW superhyperfine spectral feature of **3**. The arrow indicates the signal of the organic radical. (b) T dependence of T_1 and T_m relaxation times for **3**. The solid line is the best-fit of the model. Inset shows the room temperature data for **2** and **3**.

Good spectral simulations[26] (Figure 3a and S12) were performed on the basis of the spin Hamiltonian:

$$\mathcal{H} = \hat{\boldsymbol{I}}_V \cdot {}^V\boldsymbol{A} \cdot \hat{\boldsymbol{S}} + {}^N\boldsymbol{A} \sum_{i=1}^{4} \hat{\boldsymbol{I}}_{N_i} \cdot \hat{\boldsymbol{S}} + \mu_B \hat{\boldsymbol{S}} \cdot \boldsymbol{g} \cdot \boldsymbol{B} \qquad (2)$$

which provides as best-fit parameters the values reported in Table S2. In the EPR spectrum of **3** an additional exchange narrowed signal of an organic radical is present (Figure 3a and S12). This signal, also observed in the TiOPc matrix before and after purification (Figure S13), was assigned to the reduced species, $TiOPc^{\cdot-}$.[27] Double integration of the spectrum allowed to estimate the amount of this species as one order of magnitude less concentrate than VOPc, *viz.* 0.01% of the entire diamagnetic TiOPc. The quantities of $TiOPc^{\cdot-}$ observed in **3** and in the TiOPc diamagnetic matrix were of the same order of magnitude, thus confirming that this species is not generated as a result of the doping process.

X-band echo-detected field-swept (EDFS) EPR spectra for **3** were recorded by using a standard Hahn echo sequence (Figure 3a and S14). As evidenced by the presence of a spin-echo, we can anticipate that quantum coherence is expected for this compound. Moreover the spin Hamiltonian parameters obtained through the CW spectrum simulation allow to provide good simulations of the EDFS spectra as well, thus indicating that the entire VOPc is experiencing the detected coherence. Inversion recovery experiments were performed in the 4.3-300 K T range to investigate the T dependence of T_1 for **3** since the amount of paramagnetic component was too low for an investigation through AC susceptometry. The resulting saturation recovery traces were fitted with a standard stretched monoexponential equation (see SI) and the extracted T_1 values are reported in Figure 3b. T_1 decreases very slowly from the maximum value of ca. 14 ms at 4.3 K to 0.22 ms at 40 K in a way that is qualitatively similar to what observed for **1-2** through AC susceptometry. At higher temperature a higher slope is observed, reaching the value of 1.1 μs at room temperature. The entire curve has been simulated assuming the contribution of a direct and a Raman-like process (see SI), dominating at low and high T, respectively. Best-fit values gives a very low Raman-like exponent n of ca. 3 as already observed in closely related systems,[12,15,28] and attributed to the involvement of both optical and acoustic phonons in the relaxation.

To investigate the quantum coherence in details and to quantify the phase memory time, T_m, of VOPc in the doped material **3** as a function of T, echo decay experiments were performed at the so-called powder-like line field (345 mT) and at a lower field line (338 mT see Figure S15). Remarkably, echo decay traces (Figure 4a) were detected up to room temperature.

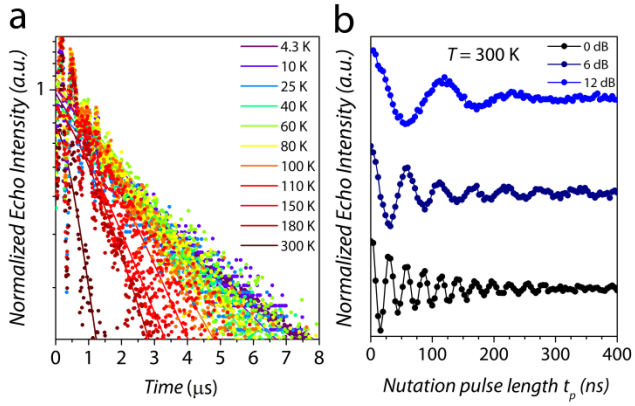

Figure 4. (a) Echo decay traces for **3** at different T (see legend). Solid lines are the best-fits (see SI). (b) Rabi oscillations recorded for **3** at 300 K for different microwave attenuations.

The thermal variation of T_m shows an almost temperature independent behavior in the 4.3-150 K range, with values within the 2.04-3.41 μs range then it slowly decreases as the

temperature increases reaching a still remarkable value of 0.83 μs at room temperature (Figure 3b). Interestingly, CuPc exhibits similar low temperature T_m but no RT coherence because of the rapid decrease of its T_1 on increasing temperature.[11] To date a slightly shorter T_m at room temperature in solid phase was obtained for $[(Ph)_4P]_2[Cu(mnt)_2]$ (mnt = maleonitriledithiolate, H-free ligand) highly diluted (0.001%) in the Ni^{II} isostructural diamagnetic host.[12] Preliminary results obtained on **2** revealed that T_1 and T_m are not suppressed by the high concentration of VOPc, assuming really remarkable values of 1.1 μs (T_1) and 0.23 μs (T_m) at room temperature (Figure 3b and S16). The observation of coherence times comparable to T_1 in concentrated and nuclear spin rich environments points out the need for strategies to decrease spin-lattice relaxation in the quest for molecular based spin qubits.

To prove that such coherence times allow to perform coherent spin manipulations *i.e.* place the spins in any arbitrary superposition of states, nutation experiments were performed at different microwave powers at 4.3 and 300 K. Remarkably, Rabi oscillations were clearly observed at room temperature for both **2** and **3**, with the expected linear dependence of the Rabi frequency, Ω_R, as a function of the B_1 relative intensity (Figure 4b and S17-S20). To the best of our knowledge, this is the first report of Rabi oscillations detected at room temperature in a molecular spin system in the solid state. Even more remarkable is their observation in a concentrated sample, indicating a particular robustness of quantum coherence in this vanadyl-based systems.

In conclusion, VOPc in its crystalline dispersion in TiOPc represents one of the few examples of potential molecular qubit showing room temperature quantum coherence. The combination of these features with its high thermal stability and high processability makes these materials extremely appealing as they can be used as paramagnetic semiconductors in spintronics devices. It is also known that VOPc molecules retain their paramagnetism when in direct contact with metallic surfaces thanks to the protected nature of the d_{xy} magnetic orbital.[17] The recent observation of EPR resonance by scanning tunneling microscopy[29] and the possibility to measure T_1 and T_m of individual atoms on surfaces further widen the interest in this vanadyl system

ASSOCIATED CONTENT

Supporting Information

Additional Figures, Tables, Equations and Experimental details as mentioned in the text. This material is available free of charge via the Internet at http://pubs.acs.org.

AUTHOR INFORMATION

Corresponding Author

roberta.sessoli@unifi.it

Notes

The authors declare no competing financial interests.

ACKNOWLEDGMENT

European Research Council (ERC) through AdG MolNanoMaS (267746), Italian MIUR through the project Futuro in Ricerca 2012 (RBFR12RPD1), and Fondazione Ente Cassa di Risparmio di Firenze are acknowledged for financial support.

REFERENCES

(1) Nielsen, M. A.; Chuang, I. L., *Quantum Computation and Quantum Information*. Cambridge Univ. Press: Cambridge, 2000.
(2) Gatteschi, D.; Sessoli, R.; Villain, J., *Molecular nanomagnets*. Oxford University Press: Oxford, UK, 2006.
(3) Troiani, F.; Affronte, M. *Chem. Soc. Rev.* **2011,** *40*, 3119-3129; Aromi, G.; Aguila, D.; Gamez, P.; Luis, F.; Roubeau, O. *Chem. Soc. Rev.* **2012,** *41*, 537-546.
(4) Ladd, T. D.; Jelezko, F.; Laflamme, R.; Nakamura, Y.; Monroe, C.; O/'Brien, J. L. *Nature* **2010,** *464*, 45-53.
(5) Kennedy, T. A.; Colton, J. S.; Butler, J. E.; Linares, R. C.; Doering, P. J. *ApPhL* **2003,** *83*, 4190-4192; Balasubramanian, G.; Neumann, P.; Twitchen, D.; Markham, M.; Kolesov, R.; Mizuochi, N.; Isoya, J.; Achard, J.; Beck, J.; Tissler, J.; Jacques, V.; Hemmer, P. R.; Jelezko, F.; Wrachtrup, J. *Nat Mater* **2009,** *8*, 383-387.
(6) Pla, J. J.; Tan, K. Y.; Dehollain, J. P.; Lim, W. H.; Morton, J. J. L.; Jamieson, D. N.; Dzurak, A. S.; Morello, A. *Nature* **2012,** *489*, 541-545.
(7) Tyryshkin, A. M.; Tojo, S.; Morton, J. J. L.; Riemann, H.; Abrosimov, N. V.; Becker, P.; Pohl, H.-J.; Schenkel, T.; Thewalt, M. L. W.; Itoh, K. M.; Lyon, S. A. *Nat Mater* **2012,** *11*, 143-147.
(8) Takahashi, S.; Tupitsyn, I. S.; van Tol, J.; Beedle, C. C.; Hendrickson, D. N.; Stamp, P. C. E. *Nature* **2011,** *476*, 76-79.
(9) Ardavan, A.; Rival, O.; Morton, J. J. L.; Blundell, S. J.; Tyryshkin, A. M.; Timco, G. A.; Winpenny, R. E. P. *Phys. Rev. Lett.* **2007,** *98*, art.n°057201; Ardavan, A.; Bowen, A. M.; Fernandez, A.; Fielding, A. J.; Kaminski, D.; Moro, F.; Muryn, C. A.; Wise, M. D.; Ruggi, A.; McInnes, E. J. L.; Severin, K.; Timco, G. A.; Timmel, C. R.; Tuna, F.; Whitehead, G. F. S.; Winpenny, R. E. P. *Npj Quantum Information* **2015,** *1*, 15012.
(10) DiVincenzo, D. P. *Fortsch. Physik* **2000,** *48*, 771-783.
(11) Warner, M.; Din, S.; Tupitsyn, I. S.; Morley, G. W.; Stoneham, A. M.; Gardener, J. A.; Wu, Z.; Fisher, A. J.; Heutz, S.; Kay, C. W. M.; Aeppli, G. *Nature* **2013,** *503*, 504-508.
(12) Bader, K.; Dengler, D.; Lenz, S.; Endeward, B.; Jiang, S.-D.; Neugebauer, P.; van Slageren, J. *Nat. Commun.* **2014,** *5*.
(13) Zadrozny, J. M.; Niklas, J.; Poluektov, O. G.; Freedman, D. E. *J. Am. Chem. Soc.* **2014,** *136*, 15841-15844.
(14) Zadrozny, J. M.; Niklas, J.; Poluektov, O. G.; Freedman, D. E. *ACS Central Science* **2015,** 10.1021/acscentsci.5b00338.
(15) Tesi, L.; Lucaccini, E.; Cimatti, I.; Perfetti, M.; Mannini, M.; Atzori, M.; Morra, E.; Chiesa, M.; Caneschi, A.; Sorace, L.; Sessoli, R. *Chem. Sci.* **2016,** 10.1039/C5SC04295J.
(16) Zhang, Y.; Learmonth, T.; Wang, S.; Matsuura, A. Y.; Downes, J.; Plucinski, L.; Bernardis, S.; O'Donnell, C.; Smith, K. E. *J. Mater. Chem.* **2007,** *17*, 1276-1283.
(17) Eguchi, K.; Takagi, Y.; Nakagawa, T.; Yokoyama, T. *The J. Phys. Chem. C* **2013,** *117*, 22843-22851.
(18) Abragam, A.; Bleaney, B., *Electron Paramagnetic Resonance of Transition Ions*. Dover: New York, 1986.
(19) Ziolo, R. F.; Griffiths, C. H.; Troup, J. M. *J. Chem. Soc., Dalton Trans.* **1980,** 10.1039/DT9800002300, 2300-2302.
(20) Duff, J. M.; Mayo, J. D.; Hsiao, C.-K.; Hor, A.-M.; Bluhm, T. L.; Hamer, G. K.; Kazmaier, P. M., Processes for the preparation of titanium phthalocyanines. Google Patents: 1992.
(21) Shrivastava, K. N. *Physica Status Solidi (b)* **1983,** *117*, 437-458.
(22) Gomez-Coca, S.; Urtizberea, A.; Cremades, E.; Alonso, P. J.; Camon, A.; Ruiz, E.; Luis, F. *Nat. Commun.* **2014,** *5*.
(23) Soeteman, J.; van Duyneveldt, A. J.; Pouw, C. L. M.; Breur, W. *Physica* **1973,** *66*, 63-69.
(24) De Vroomen, A. C.; Lijphart, E. E.; Prins, D. Y. H.; Marks, J.; Poulis, N. J. *Physica* **1972,** *61*, 241-249.
(25) Sato, M.; Kwan, T. *J. Chem. Phys.* **1969,** *50*, 558-559.
(26) Stoll, S.; Schweiger, A. *J. Magn. Reson.* **2006,** *178*, 42-55.
(27) Guzy, C. M.; Raynor, J. B.; Stodulski, L. P.; Symons, M. C. R. *Journal of the Chemical Society A: Inorganic, Physical, Theoretical* **1969,** 997-1001.
(28) Du, J.-L.; Eaton, G. R.; Eaton, S. S. *Journal of Magnetic Resonance, Series A* **1996,** *119*, 240-246.
(29) Baumann, S.; Paul, W.; Choi, T.; Lutz, C. P.; Ardavan, A.; Heinrich, A. J. *Science* **2015,** *350*, 417-420.

SYNOPSIS TOC

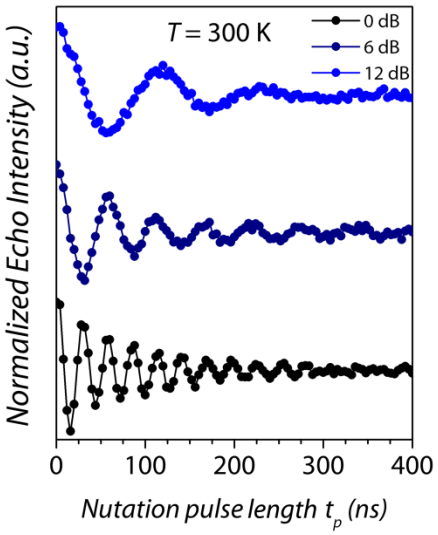

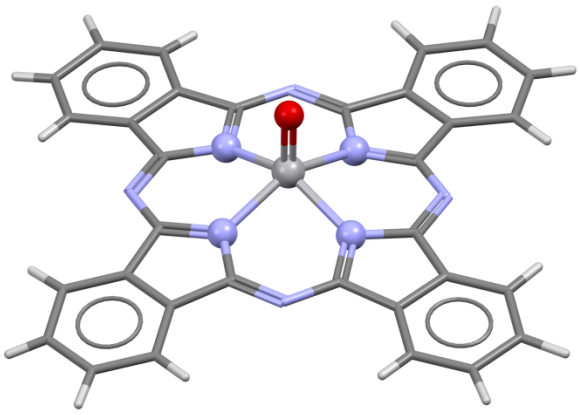

Vanadyl Phthalocyanine